# Scattering of light by bispheres with touching and separated components

Michael I. Mishchenko, Daniel W. Mackowski, and Larry D. Travis

We use the T-matrix method as described by Mishchenko and Mackowski [Opt. Lett. **19,** 1604 (1994)] to compute light scattering by bispheres in fixed and random orientations extensively. For all our computations the index of refraction is fixed at a value $1.5 + 0.005i$, which is close to the refractive index of mineral tropospheric aerosols and was used in previous extensive studies of light scattering by spheroids and Chebyshev particles. For monodisperse bispheres with touching components in a fixed orientation, electromagnetic interactions between the constituent spheres result in a considerably more complicated interference structure in the scattering patterns than that for single monodisperse spheres. However, this increased structure is largely washed out by orientational averaging and results in scattering patterns for randomly oriented bispheres that are close to those for single spheres with size equal to the size of the bisphere components. Unlike other nonspherical particles such as cubes and spheroids, randomly oriented bispheres do not exhibit pronounced enhancement of side scattering and reduction of backscattering and positive polarization at side-scattering angles. Thus the dominant feature of light scattering by randomly oriented bispheres is the single scattering from the component spheres, whereas the effects of cooperative scattering and concavity of the bisphere shape play a minor role. The only distinct manifestations of nonsphericity and cooperative scattering effects for randomly oriented bispheres are the departure of the ratio $F_{22}/F_{11}$ of the elements of the scattering matrix from unity, the inequality of the ratios $F_{33}/F_{11}$ and $F_{44}/F_{11}$, and nonzero linear and circular backscattering depolarization ratios. Our computations for randomly oriented bispheres with separated wavelength-sized components show that the component spheres become essentially independent scatterers at as small a distance between their centers as 4 times their radii.

*Key words:* Light scattering, nonspherical particles, cooperative effects, depolarization, multiple scattering.

## 1. Introduction

The scattering of light by nonspherical particles with sizes comparable to the wavelength of the incident light is a problem of significant importance to many areas of science such as atmospheric and aerosol optics, chemistry, biology, and astrophysics. In the resonance region of particle size parameters, where the Rayleigh and geometric-optics approximations are inapplicable, numerical methods for computing nonspherical scattering must be based on directly solving Maxwell's equations. The majority of computational data on light scattering by resonance nonspherical particles published so far have been obtained by the use of the T-matrix approach.[1] However, all those data pertain to convex or mildly concave single nonspherical particles such as spheroids,[2–5] finite cylinders,[6] and Chebyshev particles,[3,7] whereas it has been suggested that pronounced concavity of the particle shape or cooperative effects in composite, aggregated particles, or both, might have a strong influence on light scattering.[3,7–13] Therefore it is the aim of this paper to study light-scattering properties of the simplest aggregated particles—bispheres (two-sphere clusters)—extensively. Unlike spheroids and finite cylinders, bispheres are composite particles and, in the case of touching components, have distinctly concave shapes. On the other hand, such particles are still simple enough to allow efficient numerical computations. These two factors make bispheres well suited for an investigation of the role of cooperative effects and concavity in light scattering.

M. I. Mishchenko and L. D. Travis are with the NASA Goddard Institute for Space Studies, 2880 Broadway, New York, New York 10025. D. W. Mackowski is with the Department of Mechanical Engineering, Auburn University, Auburn, Alabama 36849-5341.

Received 9 December 1994; 27 March 1995.
0003-6935/95/214589-11$06.00/0.

The scattering of light by bispheres has been the subject of several publications (see, e.g., Refs. 9, 12, and 14 and references therein). Because of computational difficulties, essentially all published numerical results pertain to bispheres in a fixed orientation with respect to the incident beam. However, in nature small particles are usually distributed over a range of orientations rather than being perfectly aligned. Therefore computations for randomly oriented bispheres seem to be more relevant in application to natural particle ensembles and thus more suitable for deriving conclusions about the effects of particle shape on light scattering.

In a recent paper, we have developed an efficient method for rigorously computing the scattering of light by randomly oriented bispheres with sizes comparable to and larger than the wavelength.[15] The efficiency of our method is the result of combining the power of the superposition approach in treating light scattering by composite particles[8,9,14,16,17] and the analyticity of the T-matrix formulation in application to randomly oriented nonspherical scatterers.[18] The main idea of the method is to use the superposition approach to calculate the T matrix of a bisphere in the natural coordinate system with the $z$ axis connecting the centers of the component spheres and then to use this T matrix in an analytical procedure to compute the optical cross sections and the elements of the scattering matrix for randomly oriented bispheres directly. Although Ref. 15 presents only a sketch of our computational method, all intermediate steps of the derivation can easily be restored with Refs. 14, 17, and 18. Those papers contain not only the complete compendium of all necessary formulas, but also the detailed discussion of numerical aspects, which facilitates the development of an efficient computer code. As noted in Refs. 15 and 19, different parts of the code and the whole code have been extensively tested versus independent numerical data[20–22] and general equalities and inequalities that must be satisfied by the elements of the Stokes-scattering matrix,[5,23–25] as well as versus the laboratory measurements of Bottiger *et al.*[26] for randomly oriented micrometer-sized latex bispheres. The excellent quantitative agreement found in all cases allows us to believe that our code produces accurate results. Accordingly, the expected absolute accuracy of the computations of the elements of the scattering matrix reported below is better than 0.001 for all size parameters considered.

In this paper we apply our method to an extensive study of light scattering by randomly oriented bispheres. Specifically, we compute the elements of the scattering matrix and the total optical cross sections for randomly oriented bispheres with touching and separated components and compare these data with analogous computations for single spheres and bispheres in a fixed orientation. This comparison is then used to derive conclusions about the effects of aggregation and concavity on light scattering.

### 2. Bispheres with Touching Components in Fixed and Random Orientations

For all our computations we fixed the index of refraction at $1.5 + 0.005i$ based on the following rationale. First, this index of refraction is close to that of mineral tropospheric aerosols in the Earth atmosphere at visible wavelengths[27] and is, potentially, of practical interest. Second, almost the same refractive index $(1.5 + 0.02i)$ was used in previous detailed studies of light scattering by randomly oriented Chebyshev particles[3,7] and spheroids.[2,3,5] Because in this paper we extensively examine light scattering by a new class of nonspherical particles, the use of essentially the same refractive index facilitates relevant intercomparison of light-scattering properties of particles of different shape. The only purpose of slightly reducing the imaginary part of the refractive index from 0.02 down to 0.005 is to make the cooperative scattering effects for bispheres somewhat more pronounced.

The transformation of the Stokes vector of the incident light $\mathbf{I}^{\text{inc}} = [I^{\text{inc}}, Q^{\text{inc}}, U^{\text{inc}}, V^{\text{inc}}]$ into the Stokes vector of the scattered light $\mathbf{I}^{\text{sca}} = [I^{\text{sca}}, Q^{\text{sca}}, U^{\text{sca}}, V^{\text{sca}}]$ upon single scattering by a nonspherical particle in an arbitrary orientation is described by the $(4 \times 4)$ Mueller matrix $\mathbf{Z}$ as follows (Sec. 2.5 of Ref. 23):

$$\mathbf{I}^{\text{sca}} = \frac{1}{R^2} Z(\Theta)\mathbf{I}^{\text{inc}}, \tag{1}$$

where $\Theta$ is the scattering angle (i.e., the angle between the incident and the scattered beams) and $R$ is the distance between the scattering particle and the observation point. In Eq. (1), we assume that the Stokes vectors $\mathbf{I}^{\text{inc}}$ and $\mathbf{I}^{\text{sca}}$ are specified with respect to the scattering plane (i.e., the plane through the incident and the scattered beams). In general, all 16 elements of the Mueller scattering matrix are nonzero and depend not only on the scattering angle, but also on the orientation of the particle with respect to the incident and the scattered beams.

For randomly oriented particles with a plane of symmetry (such as bispheres), it is more common to use the so-called normalized (or Stokes) scattering matrix $\mathbf{F}$ given by[28]

$$\mathbf{F}(\Theta) = \frac{4\pi}{C_{\text{sca}}} \mathbf{Z}(\Theta), \tag{2}$$

where $C_{\text{sca}}$ is the scattering cross section and the (1, 1) element (i.e., phase function) satisfies the normalization condition

$$\frac{1}{4\pi} \int_{4\pi} \mathrm{d}\Omega F_{11}(\Theta) = 1. \tag{3}$$

Owing to particle symmetry and random orientation, the normalized scattering matrix has the well-known

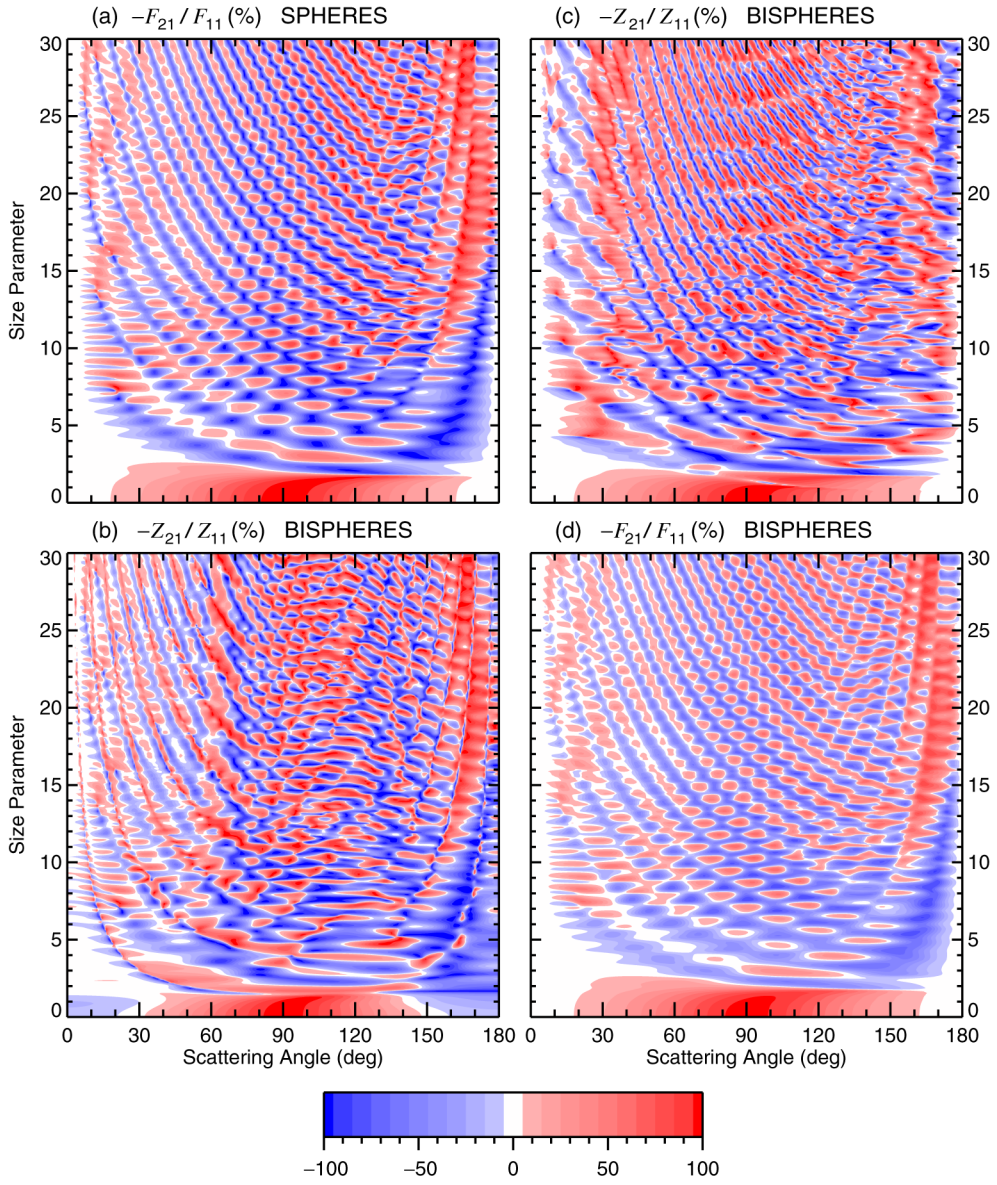


Fig. 1. Continues.

block-diagonal form[23]

$$\mathbf{F}(\Theta) = \begin{bmatrix} F_{11}(\Theta) & F_{21}(\Theta) & 0 & 0 \\ F_{21}(\Theta) & F_{22}(\Theta) & 0 & 0 \\ 0 & 0 & F_{33}(\Theta) & F_{34}(\Theta) \\ 0 & 0 & -F_{34}(\Theta) & F_{44}(\Theta) \end{bmatrix}, \quad (4)$$

so that only eight elements of **F** are nonzero and only six of them are independent.

It is well known[23,28,29] that typical features of scattering patterns for monodisperse spherical particles are so-called interference structure and high-frequency ripple, which result in strong oscillations of the optical cross sections and the elements of the scattering matrix with changing size parameter or scattering angle. Examples are given in figure 8 of Hansen and Travis[28] for the scattering cross section and figures 19 of Ref. 28 and figure 2 of Ref. 4 for the degree of linear polarization. Figure 1(a) shows the degree of linear polarization for scattering of unpolarized incident light (i.e., the ratio $-F_{21}/F_{11}$ of the elements of the Stokes-scattering matrix) for monodisperse spherical particles as a function of particle-size parameter and scattering angle. It can indeed be seen that the polarization pattern is a field of sharp local maxima and minima resulting from interference of light diffracted and reflected or transmitted by the particle.[28]

Unlike single spheres, bispheres are nonspherical particles, and the elements of the bisphere scattering matrix depend not only on the scattering angle, but also on the orientation of the particle with respect to the incident and the scattered beams. Therefore we

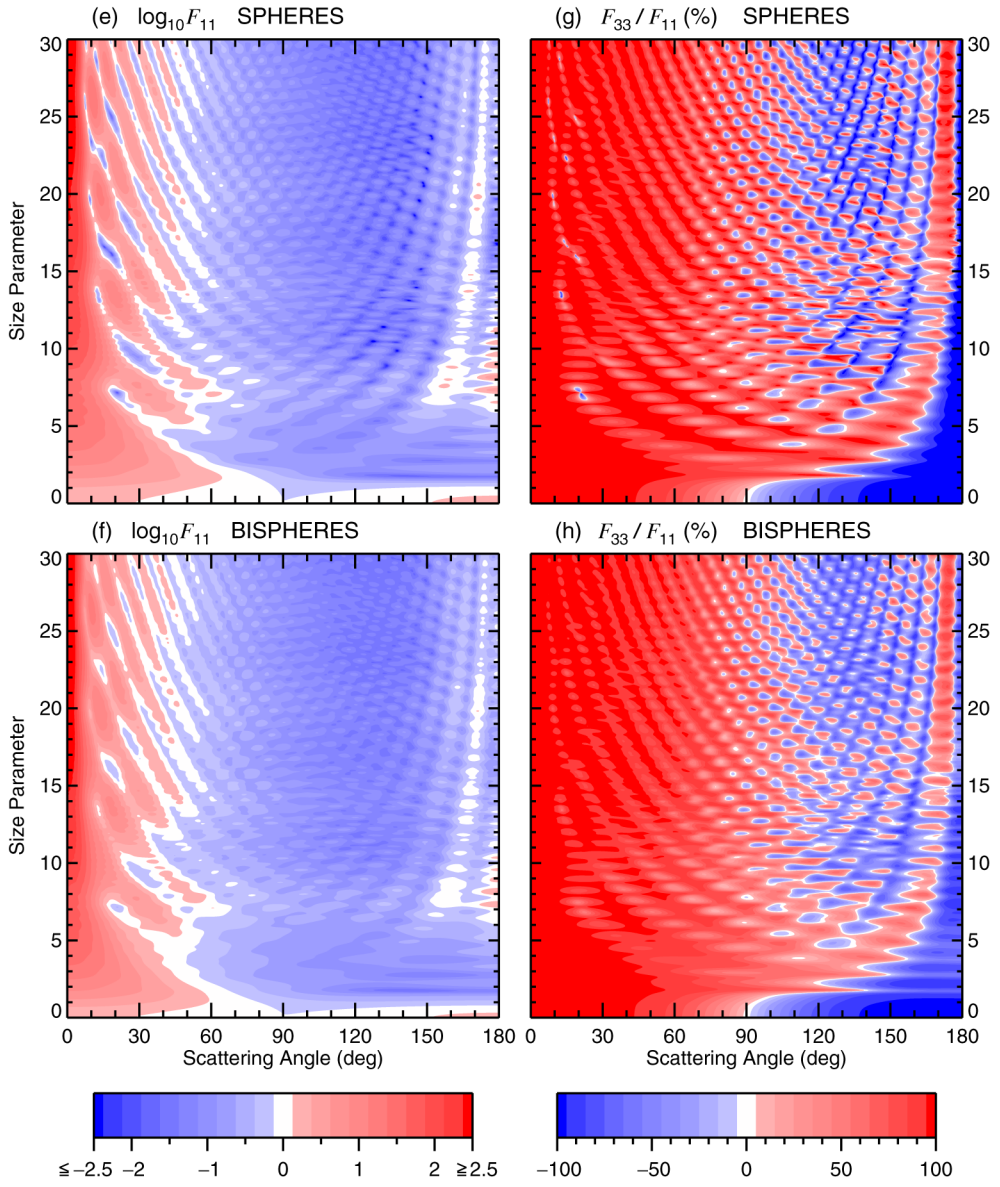


Fig. 1. Continues.

must expect that the interference structure for bispheres in a fixed orientation has an additional component that is due to the electromagnetic interaction between the constituent spheres, depends on the bisphere orientation, and is superposed on the single-sphere polarization pattern. Figures 1(b) and 1(c) show the degree of linear polarization (defined in this case as the ratio $-Z_{21}/Z_{11}$ of the elements of the Mueller-scattering matrix) as a function of the scattering angle and the constituent-sphere size parameter for two orientations of the bisphere axis (i.e., the line connecting sphere centers) with respect to the incident beam. In Fig. 1(b) the bisphere axis is perpendicular to the direction of light incidence and the scattering plane is defined as the plane through the incident beam and the bisphere axis and in Fig. 1(c) the bisphere axis is parallel to the incident beam and the scattering plane is an arbitrary plane through the incident beam. These images show that the bisphere polarization is indeed strongly dependent on the particle orientation and reveals much more complicated interference structure than the single-sphere polarization [cf. Fig. 1(a)]. In particular, the lack of axial symmetry for the light-scattering geometry in Fig. 1(b) makes polarization nonzero at 0 and, more noticeably, at 180° scattering angles. Also, the number of local maxima and minima has sharply increased. This means that in addition to the single-sphere interference structure we also have a component due to the cooperative scattering of light from constituent spheres. We should note that resolving the interference structure in Figs. 1(b) and 1(c) required size-parameter and scattering-angle step sizes of 0.05 and 0.3°, respectively.

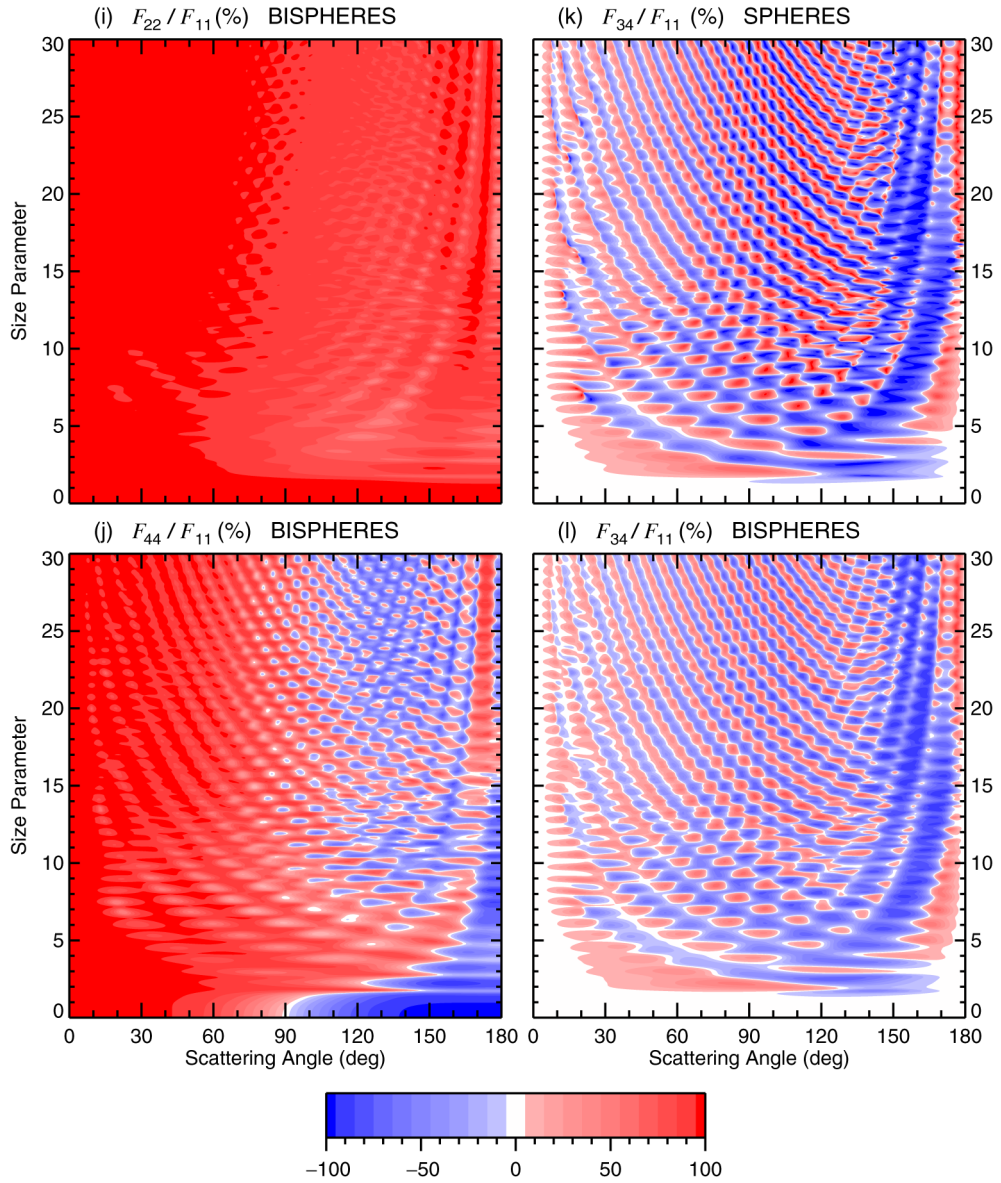


Fig. 1. (a) Ratio $-F_{21}/F_{11}$ of the elements of the scattering matrix as a function of scattering angle and size parameter for monodisperse single spheres. (b) Ratio $-Z_{21}/Z_{11}$ of the elements of the Mueller matrix as a function of scattering angle and constituent-sphere size parameter for monodisperse bispheres with touching components and axes perpendicular to the direction of light incidence. (c) Ratio $-Z_{21}/Z_{11}$ of the elements of the Mueller matrix as a function of scattering angle and constituent-sphere size parameter for monodisperse bispheres with touching components and axes parallel to the direction of light incidence. (d) Ratio $-F_{21}/F_{11}$ of the elements of the scattering matrix as a function of scattering angle and size parameter for monodisperse randomly oriented bispheres with touching components. The vertical axis shows constituent-sphere size parameters. (e) Scattering phase function $F_{11}$ as a function of scattering angle and size parameter for monodisperse single spheres. (f) As in (e) but for monodisperse randomly oriented bispheres with touching components. The vertical axis shows constituent-sphere size parameters. (g) Ratio $F_{33}/F_{11}$ of the elements of the scattering matrix as a function of scattering angle and size parameter for monodisperse single spheres. (h) As in (g) but for monodisperse randomly oriented bispheres with touching components. The vertical axis shows constituent-sphere size parameters. (i) Ratio $F_{22}/F_{11}$ of the elements of the scattering matrix as a function of scattering angle and constituent-sphere size parameter for monodisperse randomly oriented bispheres with touching components. (j) Ratio $F_{44}/F_{11}$ of the elements of the scattering matrix as a function of scattering angle and constituent-sphere size parameter for monodisperse randomly oriented bispheres with touching components. (k) Ratio $F_{34}/F_{11}$ of the elements of the scattering matrix as a function of scattering angle and size parameter for monodisperse single spheres. (l) As in (k) but for monodisperse randomly oriented bispheres with touching components. The vertical axis shows constituent-sphere size parameters.

Figure 1(d) shows the degree of linear polarization $-F_{21}/F_{11}$ computed for bispheres in random orientation. Somewhat unexpectedly, one can see a polarization pattern that is very similar to that of single spheres [Fig. 1(a)]. The only unequivocal difference is that the amplitudes of local maxima and minima are reduced, whereas the locations of the maxima and minima and their numbers are exactly the same.

This means that averaging over bisphere orientations largely washes out the second component of the interference structure and also makes the single-sphere interference structure slightly less pronounced.

Figures 1(e) and 1(f) show the scattering phase function [i.e., the (1, 1) element of the Stokes-scattering matrix] computed for single spheres and randomly oriented bispheres, and Figs. 1(g)–1(l) show the ratios $F_{22}/F_{11}$, $F_{33}/F_{11}$, $F_{44}/F_{11}$, and $F_{34}/F_{11}$ of the elements of the scattering matrix. Note that for single spheres $F_{22}/F_{11} \equiv 1$ and $F_{44}/F_{11} \equiv F_{33}/F_{11}$. Again we show that the patterns of the scattering phase function and of the ratios $F_{33}/F_{11}$, $F_{44}/F_{11}$, and $F_{34}/F_{11}$ for randomly oriented bispheres are essentially smoothed versions of those for single spheres. Specifically, the positions of the local maxima and minima and their numbers are exactly the same, although their amplitudes are somewhat reduced. This effect is also demonstrated in Figs. 2 and 3, in which the solid curves show horizontal cross sections of Figs. 1(a), 1(d), 1(e), and 1(f) corresponding to size parameters 5 and 15.

The only obvious indications of nonsphericity and cooperative scattering for bispheres are the deviation of the ratio $F_{22}/F_{11}$ from unity, the deviation of the ratios $F_{33}/F_{11}$ and $F_{44}/F_{11}$ from $-1$ at 180° scattering angle, and the inequality of the ratios $F_{33}/F_{11}$ and $F_{44}/F_{11}$. The inequality is especially noticeable at backscattering angles. Two quantities that are usually considered sensitive indicators of particle nonsphericity are the linear and the circular depolarization ratios defined as[30,31]

$$\delta_L = \frac{F_{11}(180°) - F_{22}(180°)}{F_{11}(180°) + F_{22}(180°)}, \tag{5}$$

$$\delta_C = \frac{F_{11}(180°) + F_{44}(180°)}{F_{11}(180°) - F_{44}(180°)}. \tag{6}$$

The linear depolarization ratio applies to the case of fully linearly polarized incident light and is the ratio of the cross-polarized component of the backscattered signal relative to the copolarized component. The circular depolarization ratio refers to the case of fully circularly polarized incident beam and is the ratio of the same-helicity component of the backscattered intensity relative to the opposite-helicity component. For spheres, $\delta_L \equiv 0$ and $\delta_C \equiv 0$. The depolarization ratios for randomly oriented bispheres are shown in Fig. 4. It can be seen that both $\delta_L$ and $\delta_C$ can be substantially greater than zero, especially the circular depolarization ratio. Both depolarization ratios go to zero in the limit of zero size parameter and reach maximum values at size parameters from approximately 16 to approximately 23. In the entire interval of size parameters from 0 to 30 the circular depolarization ratio is greater than the linear depolarization ratio. This result is in full agreement with the general inequality $\delta_C \geq 2\delta_L$, which is a universal characteristic of light scattering by randomly oriented rotationally symmetric particles.[32] Interestingly, the size-parameter dependence of both ratios is fully correlated: even though the ratio $\delta_L/\delta_C$ is not a size-parameter-independent constant, local maxima and minima for $\delta_L$ occur at exactly the same size parameters as those for $\delta_C$. This strongly suggests that there is a unique relationship between the linear and the circular depolarization ratios, as discussed in Ref. 32.

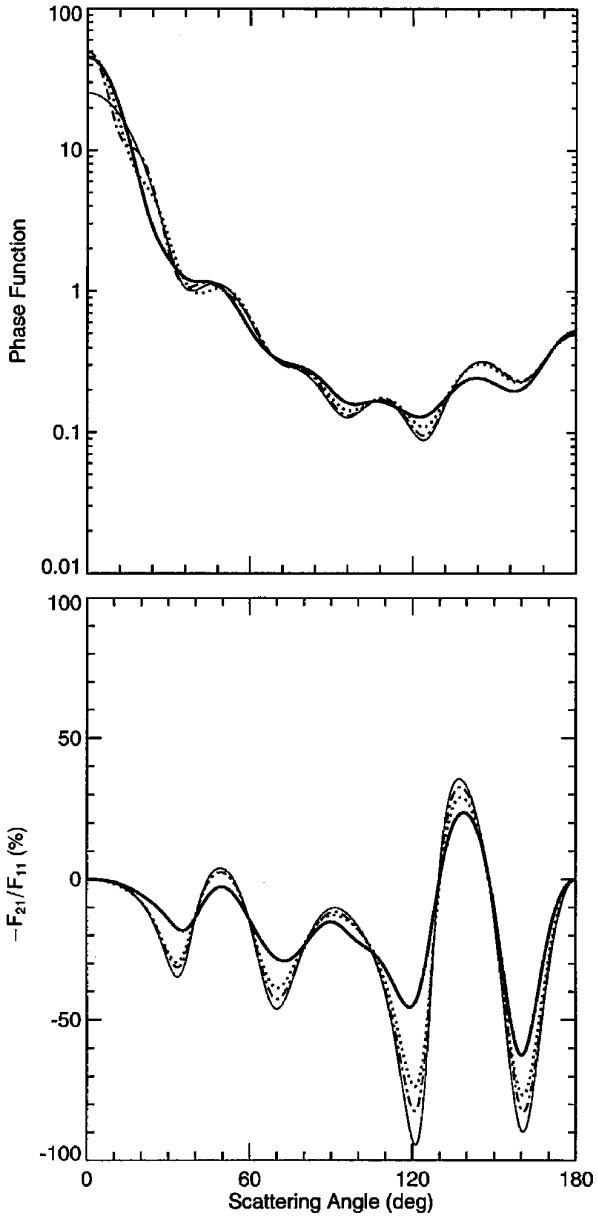


Fig. 2. Phase function and degree of linear polarization for a single sphere (thin solid curves), randomly oriented bispheres with touching components (thick solid curves), and randomly oriented bispheres with distance between sphere centers equal to 3 (dotted curves) and 4 (dotted–dashed curves) times their radius. The size parameter of the single sphere and the bisphere components is equal to 5.

Figures 5 and 6 show ratios of the total optical cross sections, single-scattering albedo, and asymmetry

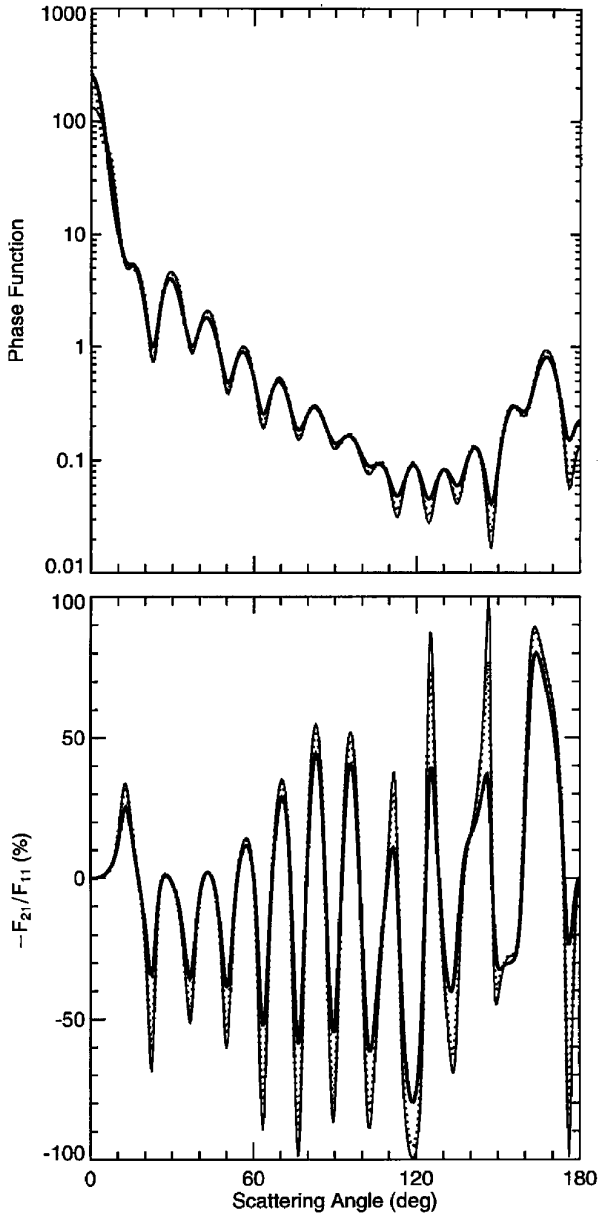


Fig. 3. Phase function and degree of linear polarization for a single sphere (thin solid curves), randomly oriented bispheres with touching components (thick solid curves), and randomly oriented bispheres with the distance between sphere centers equal to 4 times their radius (dotted curves). The size parameter of the single sphere and the bisphere components is equal to 15.

parameter of the phase function for randomly oriented bispheres relative to those for single spheres with size equal to the size of the bisphere components. Interestingly, all these ratios are nearly constant at size parameters exceeding 10. The ratio of the extinction cross sections shows both high-frequency ripple and low-frequency oscillations. However, the amplitude of the oscillations is small, and the entire curve for size parameters exceeding 6 is close to 1.8–1.85. The ratio of the orientationally averaged geometric cross section of a bisphere and the geometric cross-

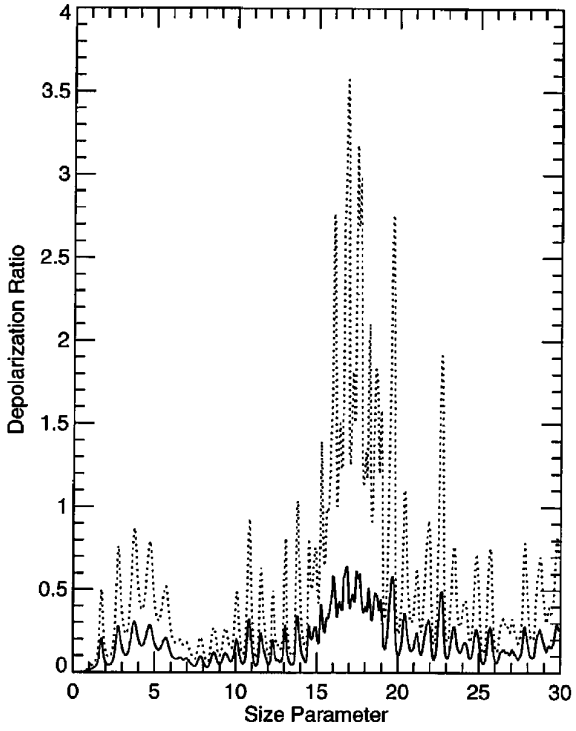


Fig. 4. Linear (solid curve) and circular (dotted curve) backscattering depolarization ratios versus constituent-sphere size parameter for randomly oriented monodisperse bispheres with touching components.

section of a sphere with size equal to the size of the bisphere components is equal to 1.849. Therefore, in the geometric-optics limit the ratio of the bisphere and single-sphere extinction cross sections must be equal to this value of 1.849. The extinction curve in Fig. 5 shows a distinct trend toward that limit with increasing size parameter. However, it is interesting that the extinction ratio is close to the geometric-optics limit even for as small a size parameter as 7.

Despite a small-amplitude high-frequency ripple, the ratio of the absorption cross sections is close to 2 at the entire range of size parameters, indicating that absorption cross section is nearly proportional to the particle volume. However, if the imaginary part of the refractive index is nonzero, then in the limit of infinite size parameter all light refracted into the particle is absorbed and does not escape. Therefore we should expect that the ratio of the bisphere and single-sphere absorption cross sections should decrease with increasing size parameter and approach the geometric cross-section ratio of 1.849. This trend can indeed be seen in Fig. 5.

The single-scattering albedo ratio is especially size parameter independent for size parameters larger than 1 and varies within a very narrow range of $1 \pm 0.02$ (Fig. 6). The asymmetry parameter ratio is also close to 1. However, all ratios but the absorption cross-section ratio rise substantially as the size parameter becomes less than 2, which demonstrates the increasing influence of cooperative scattering effects for smaller particles.

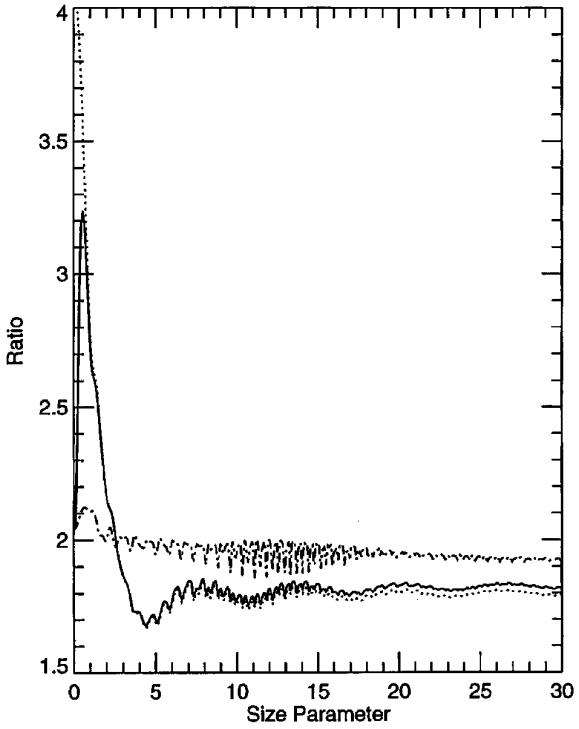


Fig. 5. Ratios of extinction (solid curve), scattering (dotted curve), and absorption (dotted–dashed curve) cross sections versus size parameter for monodisperse randomly oriented bispheres with touching components and monodisperse single spheres. For bispheres the horizontal axis shows constituent-sphere size parameters.

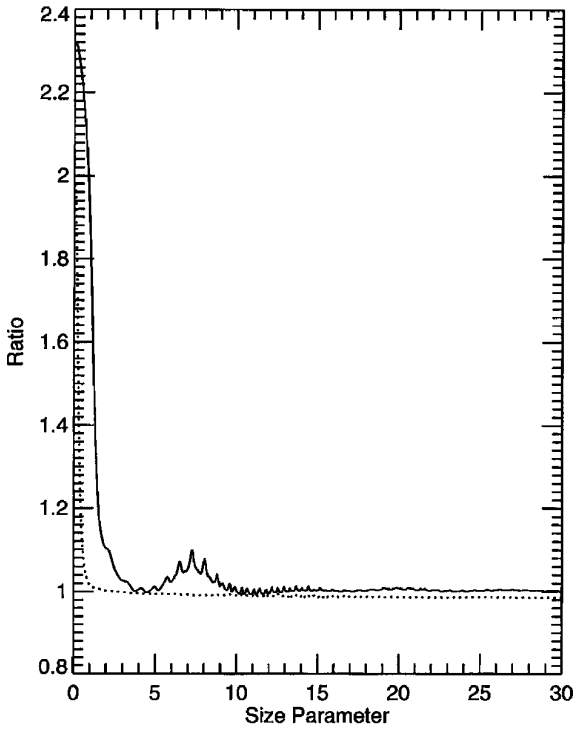


Fig. 6. Ratios of single-scattering albedos (dotted curve) and asymmetry parameters of the phase function (solid curve) versus size parameter for monodisperse randomly oriented bispheres with touching components and monodisperse single spheres. For bispheres the horizontal axis shows constituent-sphere size parameters.

### 3. Polydisperse Randomly Oriented Bispheres with Touching Components

In Section 2 we discussed light-scattering properties of monodisperse bispheres. It is well known that the main effect of averaging light-scattering characteristics over a particle-size distribution is to wash out the interference structure and ripple inherent in light-scattering patterns of monodisperse particles.[28] This effect facilitates comparison of light-scattering properties of particles with different shapes and is demonstrated in Fig. 7, in which the dotted and the solid curves show the elements of the Stokes-scattering matrix for a power-law size distribution of spheres and randomly oriented bispheres, respectively, computed at a wavelength $\lambda = 0.6283$ μm. Table 1 shows the corresponding total optical cross sections, single-scattering albedos, asymmetry parameters, and depolarization ratios. The power-law distribution is given by $n(r) \propto r^{-3}$, $r \in [r_{\min}, r_{\max}]$, with minimum and maximum radii chosen such that the effective variance of the distribution $v_{\text{eff}}$ equals 0.2 and the effective radius $r_{\text{eff}}$ equals 1 μm. The effective radius $r_{\text{eff}}$ and effective variance $v_{\text{eff}}$ are defined by equations (2.53) and (2.54) of Ref. 28 and have been shown in Refs. 5 and 28 to be the main characteristics of any physically plausible size distribution of spherical and nonspherical particles as far as light-scattering properties of particle polydispersions are concerned.

Figure 7 shows that the angular dependence of the elements of the scattering matrix for bispheres is similar to that for single spheres with effective size parameter equal to the effective bisphere monomer size parameter. The ratios $-F_{21}/F_{11}$ and $F_{34}/F_{11}$ of the elements of the scattering matrix for bispheres and single spheres are especially close. The phase functions are also close to one another except at scattering angles less than 10°, where the bisphere intensity is nearly twice that for single spheres because of constructive interference of light singly scattered by bisphere components in the forward direction. The single-scattering albedos and asymmetry parameters are essentially identical, the bisphere absorption cross section is roughly equal to twice the single-sphere absorption cross section, and the ratio of the extinction cross sections is 1.777, which is slightly less than the geometric-optics limit of 1.849. Again, manifestations of particle nonsphericity for bispheres are nonzero backscattering depolarization ratios, differences in the ratios $F_{33}/F_{11}$ and $F_{44}/F_{11}$, and the departure of the ratio $F_{22}/F_{11}$ from unity.

For comparison, the dotted–dashed curves in Fig. 7 show the elements of the scattering matrix for an equivalent power-law distribution of randomly oriented prolate spheroids with an aspect ratio of 2 and the same refractive index $1.5 + 0.005i$. The effective variance of the size distribution is $v_{\text{eff}} = 0.2$, and the

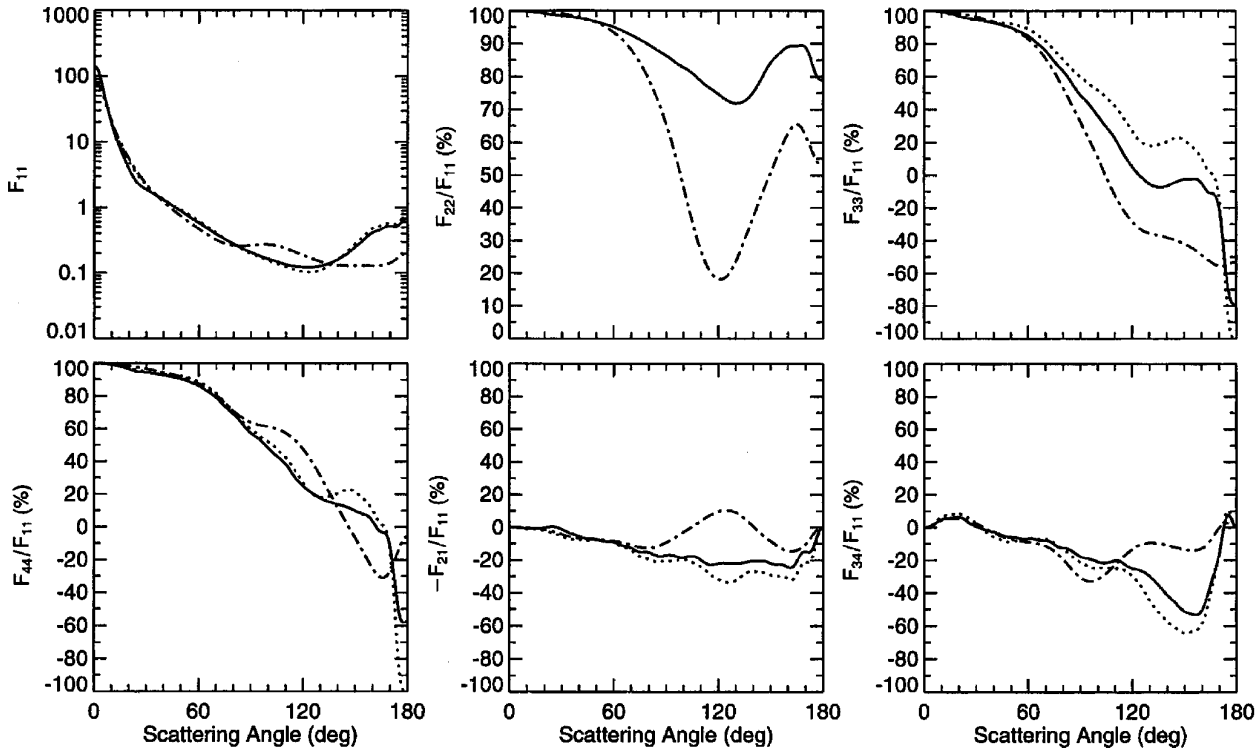


Fig. 7. Elements of the scattering matrix for polydisperse randomly oriented bispheres with touching components and effective constituent-sphere radius $r_{\text{eff}} = 1$ μm (solid curves) and polydisperse single spheres with the same effective radius (dotted curves). The effective variance of the size distribution is $v_{\text{eff}} = 0.2$ and the wavelength is 0.6283 μm. For comparison, dotted–dashed lines were computed for an equivalent power-law distribution of randomly oriented prolate spheroids with aspect ratio 2, effective variance $v_{\text{eff}} = 0.2$, and effective equal-volume-sphere radius $r_{\text{eff}} = 1$ μm.

effective equal-volume-sphere radius is $r_{\text{eff}} = 1$ μm. It is seen that, unlike the case for bispheres, the spheroidal phase function exhibits an enhanced side scattering and suppressed backscattering, and the degree of linear polarization is positive at scattering angles around 120°. Based on laboratory measurements for irregular particles[33] and nearly cubically shaped salt grains[34] and on theoretical computations for spheroids,[2,3,5,35] these features are usually considered characteristic attributes of nonspherical scattering. Spherical–nonspherical differences in the ratios $F_{22}/F_{11}$, $F_{33}/F_{11}$, $F_{44}/F_{11}$, and $F_{34}/F_{11}$ are also larger for spheres and spheroids than for spheres and bispheres.

**Table 1. Total Optical Cross Sections $C$ (in Square Micrometers), Single-Scattering Albedo ω, Asymmetry Parameter of the Phase Function ⟨cos Θ⟩, and Backscattering Depolarization Ratios for Polydisperse Randomly Oriented Bispheres with Touching Components and Effective Constituent-Sphere Radius $r_{\text{eff}} = 1$ μm and Polydisperse Single Spheres with the Same Effective Radius**[a]

| Parameter | Bisphere | Single Sphere |
|---|---|---|
| $C_{\text{ext}}$ | 8.245 | 4.641 |
| $C_{\text{sca}}$ | 7.474 | 4.247 |
| $C_{\text{abs}}$ | 0.771 | 0.394 |
| $\varpi$ | 0.907 | 0.915 |
| $\langle\cos\Theta\rangle$ | 0.724 | 0.716 |
| $\delta_L$ | 0.118 | 0 |
| $\delta_C$ | 0.268 | 0 |

[a]The effective variance of the size distribution is $v_{\text{eff}} = 0.2$, and the wavelength is $\lambda = 0.6283$ μm.

### 4. Monodisperse Randomly Oriented Bispheres with Separated Components

So far, we have discussed light scattering by bispheres with touching components. With increasing separation between constituent spheres the influence of cooperative scattering should diminish and ultimately vanish, except at exactly the forward-scattering direction. Our computations for bispheres with increasing distance between sphere centers demonstrate that this is indeed the case. As an example, Figs. 2 and 3 show the phase function and the degree of linear polarization for single monodisperse spheres and for randomly oriented monodisperse bispheres with touching and separated components. It can be seen that for essentially all scattering angles the curves for bispheres with separated components lie between the curves for single spheres and bispheres with touching components and are much closer to the single-sphere curves. In fact, it is surprising that as small a distance between the sphere centers as 4 times their radius makes the bisphere phase function and linear polarization almost identical to those of a single sphere, which means that the component spheres have become essentially independent scatter-

ers. The only exception is the direction of forward scattering, where the interference of light scattered by the bisphere components nearly doubles the phase function as compared with that for a single sphere.

## 5. Discussion and Conclusions

We have demonstrated that the scattering pattern for monodisperse bispheres with touching components in a fixed orientation is more complicated than that for single monodisperse spheres because of the additional component of electromagnetic interactions between the constituent spheres. However, averaging over the uniform orientation distribution largely washes this additional component out. The net effect of aggregation–shape concavity and random orientation for bispheres appears to be a somewhat smoothed single-sphere scattering pattern. The only distinct manifestations of nonsphericity and cooperative scattering effects for randomly oriented bispheres are the departure of the ratio $F_{22}/F_{11}$ from unity, the inequality of the ratios $F_{33}/F_{11}$ and $F_{44}/F_{11}$, and nonzero linear and circular backscattering depolarization ratios. On the other hand, despite their overall asphericity, polydisperse randomly oriented bispheres (Fig. 7) do not exhibit such characteristic features of nonspherical scattering as a considerably enhanced side scattering and suppressed backscattering as well as positive polarization at side-scattering angles.[2,3,5,33–35] Thus the dominant feature of the bisphere scattering is the single scattering from the component spheres, whereas the effects of cooperative scattering and concavity play a minor role. Moreover, this role rapidly further diminishes with increasing separation between bisphere components. As a result, the component spheres become essentially independent scatterers at as small a distance between their centers as 4 times their radii.

To explain these results we note that the effects of clustering will manifest themselves in scattering by virtue of two mechanisms, namely, near-field interactions and far-field-dependent scattering (i.e., interference between the far-field-scattered amplitudes from each sphere). For relatively larger size parameters the effects of dependent scattering between the spheres would be expected to largely cancel on orientation averaging, except at exactly the forward-scattering direction, where the interference of light singly scattered by the bisphere components is constructive regardless of the bisphere orientation. Indeed, preliminary calculations of pure dependent scattering between the spheres (in which the spheres are taken to be uncoupled in the near field, leading to $\mathbf{T}^{ij} = \mathbf{A}^{i}\delta_{ij}$ in equation 7 of Ref. 15) indicate that this is the case. The dominant effect of clustering is thus likely the result of near-field interactions. However, because large spheres scatter predominantly in the forward direction, the coupling between the spheres would have the greatest effect only for orientations in which the cluster is near parallel with the incident radiation direction. Since this specific orientation represents a relatively small fraction of all orientations, the effect of interactions will be significantly reduced on orientation averaging. In accordance with this explanation, we should expect a more pronounced influence of cooperative scattering effects for particles having sizes smaller than the wavelength and thus scattering nearly isotropically. Indeed, this increased influence can be clearly seen in Figs. 5 and 6 as a significant rise of the extinction and scattering cross sections, the single-scattering albedo, and the asymmetry parameter of the phase function as the size parameter becomes smaller than 2.

Our results are in full agreement with the conclusions of Bottiger *et al.*,[26] derived on the basis of laboratory measurements of light scattering by randomly oriented aggregates consisting of attached polystyrene spheres. They also noticed that the single-particle Mie structure was clearly evident, albeit somewhat less pronounced, in their measurements for randomly oriented aggregated particles and that the deviation of the ratio $F_{22}/F_{11}$ from unity provided the most unequivocable evidence for the nonsphericity of the aggregates. Differences between the ratios $F_{33}/F_{11}$ and $F_{44}/F_{11}$ were also noticeable, especially at backscattering angles.

Based on our results, we may anticipate that the most important factor in light scattering by a few-component cluster would be the shape of the component particles. It should be mentioned in this regard that ray-tracing computations of Macke[36] for big, randomly oriented ice crystal aggregates in the form of bullet rosettes also demonstrate that the scattering phase function for the aggregate is essentially identical to that for a single randomly oriented bullet. This has led Macke to the conclusion that multiple scattering between bullets in the aggregate plays no significant role in the overall scattering from the aggregate.

We are grateful to J. W. Hovenier and H. C. van de Hulst for valuable comments on a preliminary version of this paper and to N. T. Zakharova for help with graphics. M. I. Mishchenko and L. D. Travis thank J. E. Hansen and M. Sato for useful discussions and acknowledge partial support from the NASA Office of Mission to Planet Earth and the NASA Earth Observing System project in providing for the Earth Observing Scanning Polarimeter instrument analysis and algorithm development.

## References

1. P. C. Waterman, "Symmetry, unitarity, and geometry in electromagnetic scattering," Phys. Rev. D **3,** 825–839 (1971); P. Barber and C. Yeh, "Scattering of electromagnetic waves by arbitrarily shaped dielectric bodies," Appl. Opt. **14,** 2864–2872 (1975); V. V. Varadan, A. Lakhtakia, and V. K. Varadan, "Comment on recent criticism of the *T*-matrix method," J. Acoust. Soc. Am. **84,** 2280–2284 (1988).
2. M. I. Mishchenko, "Light scattering by size-shape distributions of randomly oriented axially symmetric particles of a size comparable to a wavelength," Appl. Opt. **32,** 4652–4666 (1993).

3. M. I. Mishchenko and L. D. Travis, "Light scattering by polydisperse, rotationally symmetric nonspherical particles: linear polarization," J. Quant. Spectrosc. Radiat. Transfer **51,** 759–778 (1994).
4. M. I. Mishchenko and L. D. Travis, "T-matrix computations of light scattering by large spheroidal particles," Opt. Commun. **109,** 16–21 (1994).
5. M. I. Mishchenko and L. D. Travis, "Light scattering by polydispersions of randomly oriented spheroids with sizes comparable to wavelengths of observation," Appl. Opt. **33,** 7206–7225 (1994).
6. F. Kuik, J. F. de Haan, and J. W. Hovenier, "Single scattering of light by circular cylinders," Appl. Opt. **33,** 4906–4918 (1994).
7. A. Mugnai and W. J. Wiscombe, "Scattering from nonspherical Chebyshev particles. 1: Cross sections, single-scattering albedo, asymmetry factor, and backscattered fraction," Appl. Opt. **25,** 1235–1244; J. Wiscombe and A. Mugnai, "Scattering from nonspherical Chebyshev particles. 2: Means of angular scattering patterns," Appl. Opt. **27,** 2405–2421 (1988).
8. F. Borghese, P. Denti, R. Saija, G. Toscano, and O. I. Sindoni, "Use of group theory for the description of electromagnetic scattering from molecular systems," J. Opt. Soc. Am. A **1,** 183–191 (1984).
9. K. Fuller, "Cooperative electromagnetic scattering by ensembles of spheres," Ph.D. dissertation (Texas A&M University, College Station, Texas, 1987).
10. R. A. West, "Optical properties of aggregate particles whose outer diameter is comparable to the wavelength," Appl. Opt. **30,** 5316–5324 (1991).
11. A-K. Hamid, I. R. Ciric, and M. Hamid, "Iterative solution of the scattering by an arbitrary configuration of conducting or dielectric spheres," IEE Proc. H **138,** 565–572 (1991).
12. K. Fuller, "Optical resonances and two-sphere systems," Appl. Opt. **30,** 4716–4731 (1991).
13. K. Lumme and J. Rahola, "Light scattering by porous dust particles in the discrete-dipole approximation," Astrophys. J. **425,** 653–667 (1994).
14. D. W. Mackowski, "Analysis of radiative scattering for multiple sphere configurations," Proc. R. Soc. London Ser. A **433,** 599–614 (1991).
15. M. I. Mishchenko and D. W. Mackowski, "Light scattering by randomly oriented bispheres," Opt. Lett. **19,** 1604–1606 (1994).
16. B. Peterson and S. Ström, "*T* matrix for electromagnetic scattering from an arbitrary number of scatterers and representations of E(3)*," Phys. Rev. D **8,** 3661–3678 (1973).
17. D. W. Mackowski, "Calculation of total cross sections of multiple-sphere clusters," J. Opt. Soc. Am. A **11,** 2851–2861 (1994).
18. M. I. Mishchenko, "Light scattering by randomly oriented axially symmetric particles," J. Opt. Soc. Am. A **8,** 871–882 (1991); **9,** 497(E) (1992).
19. M. I. Mishchenko and D. W. Mackowski, "T-matrix computations of light scattering by randomly oriented bispheres: comparison with experiment and benchmark results," submitted to J. Quant. Spectrosc. Radiat. Transfer.
20. K. A. Fuller, G. W. Kattawar, and R. T. Wang, "Electromagnetic scattering from two dielectric spheres: further comparisons between theory and experiment," Appl. Opt. **25,** 2521–2529 (1986).
21. P. J. Flatau, K. A. Fuller, and D. W. Mackowski, "Scattering by two spheres in contact: comparisons between discrete-dipole approximation and modal analysis," Appl. Opt. **32,** 3302–3305 (1993).
22. V. P. Tishkovets, "Light scattering by clusters of spherical particles. Cooperative effects under random orientation," Kinem. Fiz. Nebes. Tel. **10**(2)**,** 58–63 (1994).
23. H. C. van de Hulst, *Light Scattering by Small Particles* (Wiley, New York, 1957).
24. C-R. Hu, G. W. Kattawar, M. E. Parkin, and P. Herb, "Symmetry theorems on the forward and backward scattering Mueller matrices for light scattering from a nonspherical dielectric scatterer," Appl. Opt. **26,** 4159–4173 (1987).
25. C. V. M. van der Mee and J. W. Hovenier, "Expansion coefficients in polarized light transfer," Astron. Astrophys. **228,** 559–568 (1990).
26. J. R. Bottiger, E. S. Fry, and R. C. Thompson, "Phase matrix measurements for electromagnetic scattering by sphere aggregates," in *Light Scattering by Irregularly Shaped Particles*, D. W. Schuerman, ed. (Plenum, New York, 1980), pp. 283–290.
27. G. A. d'Almeida, P. Koepke, and E. P. Shettle, *Atmospheric Aerosols* (Deepak, Hampton, Va., 1991).
28. J. E. Hansen and L. D. Travis, "Light scattering in planetary atmospheres," Space Sci. Rev. **16,** 527–610 (1974).
29. C. F. Bohren and D. R. Huffman, *Absorption and Scattering of Light by Small Particles* (Wiley, New York, 1983).
30. K. Sassen, "The polarization radar technique for cloud research: a review and current assessment," Bull. Am. Meteorol. Soc. **72,** 1848–1866 (1991).
31. S. J. Ostro, "Planetary radar astronomy," Rev. Mod. Phys. **65,** 1235–1279 (1993).
32. M. I. Mishchenko and J. W. Hovenier, "Depolarization of light backscattered by randomly oriented nonspherical particles," Opt. Lett. (to be published).
33. R. H. Zerull, "Scattering measurements of dielectric and absorbing nonspherical particles," Beitr. Phys. Atmos. **49,** 168–188 (1976); S. C. Hill, A. C. Hill, and P. W. Barber, "Light scattering by size/shape distributions of soil particles and spheroids," Appl. Opt. **23,** 1025–1031 (1984); F. Kuik, "Single scattering of light by ensembles of particles with various shapes," Ph.D. dissertation (Free University, Amsterdam, 1992).
34. R. J. Perry, A. J. Hunt, and D. R. Huffman, "Experimental determinations of Mueller scattering matrices for nonspherical particles," Appl. Opt. **17,** 2700–2710 (1978).
35. S. Asano and M. Sato, "Light scattering by randomly oriented spheroidal particles," Appl. Opt. **19,** 962–974 (1980).
36. A. Macke, "Scattering of light by polyhedral ice crystals," Appl. Opt. **32,** 2780–2788 (1993).